# *PACS1 syndrome variant alters proteomic landscape of developing cortical organoids*

Ximena Gomez Maqueo[1], Lauren E Rylaarsdam [1], Ashley Woo [1], Annika L Schroder [1], Jennifer Rakotomamonjy [1], Shelby Ruiz [2], Jordan Gilardi[2], Lambertus Klei [2], Bernie Devlin [2], Matthew L MacDonald [2,*], Alicia Guemez-Gamboa[1,*]

[1]*Department of Neuroscience, Feinberg School of Medicine, Northwestern University, Chicago IL, USA*

[2]*Department of Psychiatry, University of Pittsburgh, Pittsburgh, PA, USA*

**Correspondence: alicia.guemez@northwestern.edu, mlmacdonald@gmail.com*

**Abstract**

PACS1 syndrome is a neurodevelopmental disorder resulting from a unique *de novo* p.R203W variant in Phosphofurin Acidic Cluster Sorting protein 1 (PACS1). *PACS1* encodes a multifunctional sorting protein required for localizing furin to the *trans*-Golgi network. Although few studies have started to investigate the impact of the PACS1 p.R203W variant, the mechanisms by which the variant affects neurodevelopment are still poorly understood. In recent years, ASD patient-derived brain organoids have been increasingly used to identify pathogenic mechanisms and possible therapeutic targets. While most of these studies investigate the mechanisms by which ASD-risk genes affect the transcriptome, studies investigating the proteome are limited. Here, we investigated the effect of PACS1 p.R203W on the proteomic landscape of brain organoids using tandem mass tag (TMT) mass-spectrometry. Time series analysis between PACS1$^{(+/+)}$ and PACS1$^{(+/R203W)}$ organoids uncovered several proteins with dysregulated abundance or phosphorylation status, including known PACS1 interactors. Although we observed low overlap between proteins with altered expression and phosphorylation, the resulting dysregulated processes converged. The presence of PACS1 p.R203W variant putatively accelerated synaptogenesis and impaired vesicle loading and recycling, putatively leading to defective and/or incomplete synaptic function. Finally, the key dysregulated proteins observed in PACS1$^{(+/R203W)}$ organoids were also enriched in ASD-risk genes and have been associated with other neurological diseases. Our results highlight that proteomic analyses not only enhance our understanding of general NDD mechanisms by complementing transcriptomic studies, but also could uncover additional targets, facilitating therapy development.

43 **Introduction**

44 Neurodevelopmental disorders (NDD) are heterogenous and usually present with complex
45 etiology. Several large-scale genetic studies into the etiology of NDDs such as autism spectrum
46 disorder (ASD), intellectual disability (ID), and epilepsy have been conducted, leading to hundreds
47 of risk genes being identified. However, our understanding of the mechanisms by which the
48 observed genetic variants act has lagged, limiting translation of genetic findings into clinical
49 treatments (1, 2). Characterizing the pathogenic mechanisms of different monogenic NDDs may
50 reveal convergent therapy targets. PACS1 syndrome (MIM615009) is a monogenic NDD
51 characterized by ASD, ID, craniofacial abnormalities, and epilepsy (3-5). PACS1 syndrome
52 results from a recurrent *de novo* c.607C>T variant in the gene encoding Phosphofurin Acidic
53 Cluster Sorting protein 1 (PACS1). This missense variant is present in all reported patients and
54 results in an arginine to tryptophan (p.R203W) substitution at residue 203, with only one known
55 arginine to glutamine p.R203Q exception (5).

56 *PACS1* encodes a multifunctional sorting protein required for furin localization to the *trans*-
57 Golgi network (tGN) (6, 7). PACS1 binds furin and other targets via acidic cluster sorting motifs
58 (8-11). In addition to tGN retrieval, PACS1 mediates the recycling of endocytosed furin from early
59 endosomes to the cell surface and the delivery of proteins to the primary cilium (12-14). PACS1
60 has been shown to interact with over 50 other proteins (10, 14-17). Although the role of PACS1
61 has primarily been studied in the cytoplasm, several reports show that it also accumulates in the
62 nucleus (18, 19) where it mediates DNA replication repair (20, 21), contributes to the nuclear
63 export of viral transcripts (18), and regulates chromatin stability through interaction with histone
64 deacetylase (HDAC) proteins (20).

65 Recent reports have begun to explore the pathogenesis of the PACS1 p.R203W variant.
66 Mice overexpressing PACS1 p.R203W exclusively in cortical neurons present with increased
67 dendrite arborization and decreased postsynaptic currents, possibly due to a pathogenic
68 interaction between PACS1 p.R203W and HDAC6. Moreover, antisense oligonucleotides (ASO)

69 directed towards both PACS1 and HDAC6 ameliorate these defects (22). Transcriptomic analysis
70 in patient-derived brain organoids revealed a dysregulation in cell projection organization in
71 immature PACS1 p.R203W neurons, while mature neurons exhibited an upregulation in synaptic
72 signaling processes when compared to isogenic controls. Subsequent characterization of
73 spontaneous electrical activity revealed that induced pluripotent stem cell (iPSC)-derived neurons
74 harboring the p.R203W variant display asynchrony and an increased network burst duration (23).
75 Finally, a study using *C. elegans* showed that the PACS1 syndrome-associated variant altered
76 PACS1 localization but had no effect on neuron morphology and synaptic patterns (24). Although
77 these studies have started to investigate the impact of the PACS1 p.R203W variant, the
78 mechanisms by which the variant affects neurodevelopment are still poorly understood. This in
79 turn results in few therapeutic for patients, which include only non-invasive behavioral approaches
80 and sensory integration therapies to manage the symptoms (25, 26).

81 In recent years, ASD patient-derived brain organoids have been increasingly used to
82 identify pathogenic mechanisms and possible therapeutic targets (27). While most of these
83 studies investigate the mechanisms by which ASD-risk genes affect the transcriptome (28, 29),
84 studies investigating the proteome are limited. However, mRNA levels do not always predict
85 protein levels, as protein expression and degradation are regulated by mechanisms beyond
86 transcription (30). Here we used tandem mass tag (TMT) mass-spectrometry to provide further
87 understanding into the pathogenic mechanisms of PACS1 syndrome by uncovering whether brain
88 organoids carrying the unique PACS1 p.R203W variant present with a dysregulated proteomic
89 landscape during maturation.

90

91 **Methods**

92 ***Generation of forebrain organoids from iPSCs***

93 Three isogenic pairs of PACS1$^{(+/+)}$ and PACS1$^{(+/R203W)}$ iPSC lines were previously generated (23)
94 and differentiated to brain organoids using the kit based on Sloan et al. protocol (31) (Stem Cell

95 Technologies, 08620). See Supplementary Methods for further details on organoid generation
96 and immunostaining.
97
98 **Sample preparation for proteomic analysis**
99 Total protein was extracted from the organoids by sonication in lysis buffer (1% sodium dodecyl
100 sulfate (SDS), 125 mM triethylammonium bicarbonate (TEAB), 75 mM NaCl, and HaltTM protease
101 and phosphatase inhibitors). Lysate samples from two additional control cell lines were included
102 to improve protein detection. See Supplemental Methods and Supplementary Table 1 for detailed
103 description of the mass spectrometry sample preparation, TMT labeling and phosphopeptide
104 enrichment processing steps.
105
106 **MS data acquisition and raw data processing**
107 For peptide/protein quantification, TMT labeled peptides (~1 µg) were loaded onto a heated
108 PepMap RSLC C18 2 µm, 100 angstrom, 75 µm x 50 cm column (Thermo Scientific) and eluted
109 over 180 min gradients optimized for each high pH reverse-phase fraction (32). Sample eluate
110 was electrosprayed (2000 V) into a Thermo Scientific Orbitrap Eclipse mass spectrometer for
111 analysis. MS1 spectra were acquired at a resolving power of 120,000. MS2 spectra were acquired
112 in the Ion Trap with CID (35%) in centroid mode. Real-time search (max search time = 34 s; max
113 missed cleavages = 1; Xcorr = 1; dCn = 0.1; ppm = 5) was used to select ions for synchronous
114 precursor selection for MS3. MS3 spectra were acquired in the Orbitrap with HCD (60%) with an
115 isolation window = 0.7 m/z and a resolving power of 60,000, and a max injection time of 400ms.
116 For phosphopeptide quantification, 4 µl (out of 20) of the TMT labeled phosphopeptide
117 enrichments were loaded onto a heated PepMap RSLC C18 2 µm, 100 angstrom, 75 µm x 50 cm
118 column (Thermo Scientific) and eluted over a 180 min gradient: 1 min 2% B, 5 min 5% B, 160 min
119 25% B, 180 min 35% B. Sample eluate was electrosprayed (2000 V) into a Thermo Scientific

120 Orbitrap Eclipse mass spectrometer for analysis. MS1 spectra were acquired at a resolving power
121 of 120,000. MS2 spectra were acquired in the Orbitrap with HCD (38%) in centroid mode with an
122 isolation window = 0.4 m/z, a resolving power of 60,000, and a max injection time of 350 ms.

123

124 The raw MS files were processed using Proteome Discoverer version 2.4 (Thermo Scientific,
125 Waltham, MA). MS spectra were searched against the *Homo sapiens* Uniprot/SwissProt
126 database. SEQUEST search engine was used (enzyme = trypsin, max. missed cleavage = 4, min.
127 peptide length = 6, precursor tolerance = 10 ppm). Static modifications include carbamidomethyl
128 (C, +57.021 Da), and TMT labeling (N-term and K,+304.207 Da for TMTpro16). Dynamic
129 modifications include oxidation (M, +15.995 Da), Phosphorylation (S, T, Y,+79.966 Da, only for
130 phosphopeptide dataset), acetylation (N-term,+ 42.011 Da), Met-loss (N-term, –131.040 Da), and
131 Met-loss + Acetyl (N-term, –89.030 Da). PSMs were filtered by the Percolator node (max Delta
132 Cn = 0y .05, target FDR (strict) = 0.01, and target FDR (relaxed)=0.05). Proteins were identified
133 with a minimum of 1 unique peptide and protein-level combined q values < 0.05. Reporter ion
134 quantification was based on corrected S/N values with the following settings: integration tolerance
135 = 20 ppm, method = most confident centroid, co-isolation threshold = 70, and SPS mass matches
136 = 65.

137

138 ***Bioinformatic processing***

139 Protein intensity data values were first normalized to adjust each TMT experiment to an equal
140 signal per channel. A global scaling value and the internal reference scaling factor were then
141 calculated (33), after which a median normalization was performed and then log2-transformed.
142 Further analysis of the data indicated a strong batch effect associated to the multiplex labeling,
143 which we ameliorated with the function removeBatchEffect in the R package limma (v3.58.0) (34).
144 The experimental variability associated to the genotype, day, isogenic cell line, and differentiation

145 variables were retained in the design matrix. Only the proteins (Supplementary Table 2 and 3)
146 and phosphopeptides (Supplementary Table 4 and 5) present in all plexes were used for
147 downstream analysis. This stringent filter was implemented to better control batch effects and
148 addressed the impossibility of differentiating the missing values from non-expressed proteins.
149 Despite this stringent filter, we captured a diverse pool of proteins and phosphopeptides similar
150 to other publicly available datasets (27).

151

152 *Time series clustering*. We used the Short Time-series Expression Miner software (STEM,
153 v1.3.13;) (35), which compares and assigns each expression profile from the dataset to a set of
154 distinct and representative models of temporal expression profiles based on the total timepoints.
155 These model profiles are independent of the data and correspond to possible profiles of a protein's
156 change in expression over time. For its implementation, the batch-corrected normalized protein
157 abundances in the organoids were first log2-transformed and averaged by isogenic line and
158 timepoint. We also used a fetal brain proteome previously reported by Djuric *et al*. (36) and
159 selected the prenatal samples from all reported brain regions (ventricular zone, intermediate zone,
160 subplate zone and cortex). The fetal brain samples were processed using each region as a
161 replicate for clustering. The STEM algorithm then transforms all trends to start at 0, generating a
162 vector (0, $v_1 — v_0$, $v_2 — v_0$, …, $v_n — v_0$) for each protein. Proteins are then assigned to the model
163 profile to which their time series most closely matches based on correlation coefficient. The
164 number of proteins assigned to each model profile is then tested for statistical significance against
165 the number of proteins expected to be assigned to a profile. This number is estimated by randomly
166 permuting the original time points, renormalizing the protein abundances, and then assigning
167 them to the most closely matching model profiles. The average number of proteins assigned to a
168 model profile over all permutations was used as the estimate of the expected number of genes
169 assigned to the profile. This process was performed using a significance level of 0.05 of the

170 Bonferroni-corrected p-value. The values used for each parameter are presented in
171 Supplementary Table 6. Several preliminary runs were performed to select the values that both
172 offered clustering of most proteins and diversity of profiles, while also controlling for the number
173 of highly similar profiles. Protein overlap among analyzed datasets were performed using the
174 packages GeneOverlap (v.1.40.0) (37) and UpSetR (v.1.4.0) (38).

175

176 *Functional processes – Gene enrichment analysis.* Testing for enrichment was performed with
177 the online tool Metascape (v3.5.20240901) (39), using a hypergeometric test followed by the
178 Benjamini-Hochberg *p*-value correction, selecting statistically significant terms at a cutoff value
179 below -1.3 Log(q-value) (39), and then simplifying redundancy in the resulting lists using rrvgo in
180 R (v1.16) (40). Enrichment tests were performed using the Gene Ontology (GO) biological
181 processes (41, 42) and the gene-disease association DisGeNET (43) databases. Visualizations
182 were performed using webr (v.0.1.5) (44) and ggplot2 functions (v3.5.1) (45). The GO-term
183 network was performed in Metascape. In brief, the 20 top-score clusters (lowest p-values) were
184 selected from each dysregulated expression trend and then used the Kappa similarity statistic
185 above 0.3 to connect similar terms (39). The resulting network was then edited in Cytoscape
186 (v3.10.2) (46). Additionally, we queried the SFARI Gene database (2024 Q3 release) (47) to
187 detect dysregulated genes that have also been linked to ASD.

188

189 **Results**

190

191 ***Brain organoids capture proteomic developmental trajectories and processes observed in***
192 ***fetal brain***

193 Proteins are the ultimate effectors of the cellular processes, thus, here we characterized the
194 proteome of iPSC-derived brain organoids to better understand how p.R203W PACS1 impacts

195 neurodevelopment. Organoids were collected at distinct differentiation time points: day 21, when
196 proliferating neural precursors predominate; day 40, when some progenitors have transitioned
197 into intermediate progenitors and newly born neurons; and day 90, when post-mitotic neurons are
198 the most abundant population (Fig. 1A).

199 We utilized TMT mass-spectrometry to detect 3,766 unique proteins in our organoids
200 across stages, with ~60% overlapping with proteins present in fetal brains (Fig. S1A). Most
201 overlap was observed within organoids and brain samples from post-conception week 16 through
202 26, with protein abundance correlation increasing with organoid maturation (Fig. S1B). We first
203 aimed to understand the proteomic landscape of maturing organoids derived from neurotypical
204 iPSCs. We identified groups of proteins with common temporal trajectories by performing time
205 series and clustering analysis. We classified proteins into three temporal patterns: upregulation,
206 downregulation, and stable abundance over time. The up and downregulated patterns were
207 further clustered into two main profiles: 1) continuous protein change, with steady
208 increase/decrease in abundance (clusters “steady-up” and “steady-down”); and 2) delayed trend,
209 where protein abundance remained stable from day 21 to day 40, and then increased/decreased
210 at day 90 (clusters “delayed-up” and “delayed-down”) (Fig. 1B; Supplementary Table 6).

211 Next, we used gene ontology (GO) analysis to determine the biological processes involved
212 within these distinct patterns (Supplementary Table 7). As expected, many developmental
213 processes changed with time: cell migration, neuron projection, and synaptic function were
214 upregulated (Fig. 1C, outer circle), while neurogenesis was downregulated (Fig. 1D, outer circle).
215 This is consistent with the differentiation from neural precursor to neurons as the organoids
216 mature. Within the upregulated clusters, the steady-up contained most of the neurodevelopmental
217 processes, while the delayed-up was mostly associated with signaling. Likewise, clusters steady-
218 down and delayed-down shared a downregulation of cell cycle and differentiation (Fig.1D). Stable
219 proteins were associated with basic functions like primary metabolism, regulation of gene
220 expression, and ribosome/translation-related processes (Fig. S1C).

221 Finally, we compared the observed organoid processes with the developing fetal brain
222 dynamics obtained from a reference dataset (36) (Fig. S1D and Supplementary Table 8). We
223 found significant overlaps between clusters in organoids with the same temporal patterns in the
224 fetal brain (Supplementary Table 9). In addition, most of the enriched processes during brain
225 development were captured in the corresponding pattern by the organoids. These results confirm
226 that our brain organoids recapitulate early stages of brain development, as previously reported
227 (27), supporting their use to model protein dysregulation in PACS1 syndrome.
228
229 ***PACS1 p.R203W pathogenic variant putatively accelerates axonal and synaptic maturation***
230 We then profiled the proteome of PACS1 syndrome patient-derived brain organoids to evaluate
231 the effects of the PACS1 p.R203W pathogenic variant on protein regulation during development
232 (Fig. 1A). Maturation time was the strongest driver of variance when comparing PACS1$^{(+/+)}$ and
233 PACS1$^{(+/R203W)}$ organoids at days 21, 40, and 90 using principal component analysis (PCA, 42%
234 of variation) (Fig. S2). We investigated whether the presence of the PACS1 variant impacts
235 groups of proteins that share common temporal trajectories. PACS1$^{(+/R203W)}$ organoids also
236 presented with the three major patterns (upregulation, downregulation, and stable) and profiles
237 (steady vs. delayed) observed in controls (Fig. 2A, Supplementary Table 10). However, several
238 proteins switched abundance patterns (Fig. 2B). The profile rearrangement resulted in four
239 additional clusters, for a total of eight clusters found in PACS1$^{(+/R203W)}$ organoids. These clusters
240 included proteins that were up or down-regulated when compared to the stable pattern in controls
241 ("stable-up" and "stable-down" clusters), or that lost the regulation observed in controls and
242 remained stable over maturation ("up-stable" and "down-stable" clusters; Supplementary Table
243 11).
244 The stable-up cluster from PACS1$^{(+/R203W)}$ organoids had an enrichment in processes like
245 axon projection, neuron projection guidance, and post-synapse organization (Fig. 2C). Proteins
246 that gain upregulation included the microtubule-associated protein MAP1S, required for neurite

247 extension (48); the transmembrane ligand ephrin B3, involved in synapse and spine formation
248 (49); and the histone deacetylase HDAC5, a potential PACS1 interactor involved in axon growth
249 and regeneration (50) (Supplementary Table 12). On the other hand, the stable-down cluster
250 showed enrichment of known PACS1 functions associated to viral transcripts trafficking (18), as
251 well as translation at synapses and RNA processing. Proteins that gain downregulation included
252 ribosomal subunit proteins such as RPL15 and RPS10, and spliceosomal complex assembly
253 proteins. In this cluster we also detected known PACS1 interactors including the phosphatase
254 subunit PPP1CA, essential for cell division and a regulator of neuronal differentiation and synaptic
255 transmission (51); and the IGF2R/CI-MPR receptor, involved in intracellular trafficking of
256 lysosomal enzymes (52) and recently implicated in neurodegenerative disorders (53).

257 The down-stable cluster was also enriched in translational elongation and alternative
258 splicing, with the broader "protein translation" category overlapping with the stable-down cluster.
259 However, the nested terms in this category suggest that there could be a shift in the location
260 where active translation is occurring in PACS1$^{(+/R203W)}$ organoids, decreasing at the synapse while
261 retaining it at the mitochondria. Proteins that lost their temporal downregulation and remained
262 stable over time included known PACS1 interactor CSNK2A2, the catalytic subunit alpha 2 of
263 casein kinase 2 (CK2). Interestingly, CSNK2A2 is not only activated by PACS1 but also enhances
264 PACS1 cargo-shuttling function by direct phosphorylation (52).

265 Finally, the up-stable cluster was enriched in processes related to vesicle recycling and
266 cargo loading at synapses, and Golgi organization and transport. Proteins that lost their temporal
267 upregulation and remained stable in PACS1$^{(+/R203W)}$ organoids included the secreted glycoprotein
268 WNT7A, involved in regulating protein localization at the pre-synapse and preferentially
269 stimulating excitatory synapse formation and function (54); as well as the transmembrane
270 trafficking proteins TMED2, TMED3, and TMED4, required for Golgi apparatus organization and
271 localization of proteins to the plasma membrane (55). As in the other clusters, we found a known
272 PACS1 interactor, the Golgi-associated gamma-adaptin GGA3. Notably, GGA3-mediated

273 trafficking is regulated not only by its interaction with PACS1 but also with CK2 (that lost its
274 temporal regulation and remained stable in PACS1$^{(+/R203W)}$ organoids) (52). Other proteins that
275 lost regulation over time, including the kinesin KIF5C, the ATPase TOR1A, and a component of
276 the coat protein complex II (COPII) SEC31A, are implicated in synaptic maturation through vesicle
277 loading and recycling.

278 Our results uncovered dysregulation of known interactors of PACS1 on the protein level
279 that were not resolved on the transcriptome level (23). Results suggest that the PACS1$^{(+/R203W)}$
280 organoids could present with accelerated development, with the upregulation of processes related
281 to establishing cell polarity, axon growth, and synapse maturation. However, even if the
282 PACS1$^{(+/R203W)}$ organoids present with early synaptic formation signatures, they also lost
283 regulation of many synaptic processes, like vesicle loading and recycling, that could lead to
284 defective and/or incomplete synaptic function (Supplementary Table 13).

285

286 ***Temporally regulated phosphorylation of proteins related to axonal and synaptic***
287 ***processes are also impacted in PACS1$^{(+/R203W)}$ brain organoids***

288 Post-translational phosphorylation is a main regulator of protein function. Thus, we analyzed
289 whether the PACS1$^{(+/R203W)}$ organoids also presented with alterations in phosphorylation during
290 maturation. Quantification of phospho-peptides in organoids resolved a total of 4,238
291 phosphorylation sites. The time series and clustering analysis uncovered the same eight clusters
292 and stable patterns that resulted from the protein abundance analysis (Fig. 3A, Supplementary
293 Tables 14-16). However, an additional distinct cluster composed of peptides that acquired
294 phosphorylated sites between days 21 and 40 ("early-up" cluster) was observed in PACS1$^{(+/R203W)}$
295 organoids (Fig. 3B).

296 A total of 554 phosphorylation sites on 347 unique proteins were dysregulated in
297 PACS1$^{(+/R203W)}$ organoids (Supplementary table 17). Examples include two PACS1 known
298 interactors, PACS2 (PACS1 paralog) and HDAC1. PACS1$^{(+/R203W)}$ organoids presented with

299 increased PACS2-S437 phosphorylation, which is required for PACS2-mediated trafficking and
300 repression of apoptosis (56). HDAC1 had decreased phosphorylation at residues S421 and S423
301 which is essential for its repressive function (57). Interestingly, both serine residues are also
302 phosphorylated by CK2 (found to have lost its temporal regulation and remaining stable in
303 PACS1$^{(+/R203W)}$ organoids).

304 Because phosphorylation could result either in an induction or inhibition of protein function,
305 and the activation status of a protein itself could have diverse effects on pathway activity, we used
306 the Phosphosite database to understand the functional impact of the observed dysregulated
307 phosphorylation sites (58). Phosphosite contained annotations on 51 out of 554 phosphorylation
308 sites across 41 unique proteins, with few proteins having multiple phosphorylated sites (Fig. S3,
309 Supplementary Table 19). To perform the functional enrichment analysis, we grouped
310 phosphorylated proteins that gained (clusters: stable -up and -down) or lost (clusters up- and
311 down-stable) phosphorylation regulation in contrast to the controls. Although the early-up cluster
312 also gained upregulation, due to its uniqueness to this dataset, we performed the functional
313 enrichment analysis separately (Fig. 3C, Supplementary Table 18).

314 The phosphorylated proteins that gained up/down- regulation in the PACS1$^{(+/R203W)}$
315 organoids over time while remaining stable in controls are involved in axonogenesis, as well as
316 synaptic function and organization processes (Fig. 3C, orange pie plot). Examples of these
317 proteins include synapsin1 (SYN1), implicated in both synaptogenesis and neurotransmitter
318 release, whose phosphorylation at residues S568/S570 causes conformational changes that
319 prevents its binding to actin or synaptic vesicles (59); synaptojanin1 (SYNJ1) which has a
320 prominent role in synaptic vesicle recycling (60); the beta subunit of the AP-3 protein complex, a
321 known PACS1 interactor, that helps form clathrin-coated synaptic vesicles (60); and DNM1-S774,
322 which regulates clathrin-mediated endocytosis through its activation by dephosphorylation (61).

323 Similarly, as observed in the other gain of regulation clusters, the early-up cluster had
324 enrichment for axon-related function and organization, but showed novel terms related to

325 signaling through semaphorin 3 (SEMA3E) (Fig. 3C, green pie plot). This result is in consensus
326 with single-cell RNA sequencing analysis, which identified *SEMA3E* to be upregulated in
327 PACS1$^{(+/R203W)}$ brain organoids (23). Our proteomic dataset shows that while there are no changes
328 in SEMA3E, several proteins involved in its signaling pathway are phosphorylated, including
329 CRMP1, DPYSL2 and DPYSL3. DPYSL2-S522 phosphorylation by CDK5 is involved in axonal
330 guidance and spine development (62).

331 Meanwhile, intracellular protein transport was the most enriched process in the clusters
332 that lost regulation (Fig. 3C, brown pie plot). Proteins that remained stable in PACS1$^{(+/R203W)}$
333 organoids include GLI3, which has a dual function as a transcriptional activator and a repressor
334 of the sonic hedgehog (Shh) pathway dependent on phosphorylation (63); and LIN28A, an RNA-
335 binding protein that is localized to the peri-endoplasmic reticulum and has been recently described
336 as a global suppressor of genes in the secretory pathway (64).

337

338 ***Dysregulated protein abundance and phosphorylation status in PACS1$^{(+/R203W)}$ organoids***
339 ***result in convergent processes and overlap with known NDD-related genes***

340 We next analyzed the overlap of protein identities with dysregulated abundance and
341 phosphorylation status in PACS1$^{(+/R203W)}$ organoids. Surprisingly, we observed a low overlap of
342 both the total and dysregulated proteins identified in both datasets (Fig. 4A, B). Nevertheless,
343 most affected processes converged (Fig. S4). For example, axon- and synapse- related
344 processes, as pointed out in the previous sections, are enriched due to dysregulated abundance
345 and phosphorylation status over time in PACS1$^{(+/R203W)}$ organoids when compared to controls
346 (purple and yellow). This is the case for most of the observed processes including protein
347 transport, cytoskeleton organization, and cell cycle. Some exceptions include processes like
348 energy metabolism that comes from the dysregulation of protein abundance (purple) and neuron
349 migration, which is composed of proteins showing a gain of upregulation in phosphorylation status

350 over time (yellow). These results suggest that PACS1$^{(+/R203W)}$ organoids development is disrupted
351 at different regulation levels.

352 Next, we investigated whether there are convergent dysregulated proteins in PACS1
353 syndrome compared to other NDDs. We performed gene-set enrichment analysis on the
354 dysregulated proteins using the DISGENET and the Simons Foundation ASD (SFARI) gene
355 databases. A total of 241 genes (20%) dysregulated in the PACS1$^{(+/R203W)}$ organoids compared to
356 controls are also reported in these databases. In DISGENET, we found 160 genes that showed
357 a significant enrichment in multiple nervous system disorders (Fig. 4A; Supplementary Table 20).
358 These disorders overlapped with phenotypes observed in PACS1 syndrome patients like ASD,
359 ID, seizures, and abnormal morphogenesis of the nervous system or facial features (3, 65), as
360 well as phenotypes yet to be reported like neurodegeneration. Finally, 117 of the genes that we
361 identified to be dysregulated in PACS1$^{(+/R203W)}$ organoids are also reported as ASD-risk genes in
362 the SFARI database (Fig. 4B, Supplementary Table 21). These results support the overlap of
363 PACS1 syndrome and dysregulated processes with ASD and expand on phenotypes that patients
364 could manifest later in life.

365

366 **Discussion**

367 NDDs are highly heterogenous and can arise from variants across hundreds of genes (57,
368 58). However, several limitations have hampered our understanding of the mechanisms by which
369 these variants act, limiting translation of genetic findings into the clinic (59, 60). Here we leveraged
370 the potential of brain organoids to model neurodevelopment and gain insights into the pathogenic
371 mechanisms of PACS1 syndrome. By using mass spectrometry with TMT, we identified 7,230
372 unique proteins, of which 3,677 were quantified with 100% present call in our samples, a yield
373 consistent with findings from other proteomic studies involving brain organoids (27, 61, 62).
374 Moreover, we observed temporal trajectories that reflected the transitions from proliferating

375 progenitor cells towards mature neuronal lineages, mimicking the temporal dynamics observed in
376 the fetal brain.

377 PACS1$^{(+/R203W)}$ organoids presented with dysregulated abundance and phosphorylation
378 status of temporally regulated proteins, including PACS1 known interactors. Despite the low
379 overlap between expression and phosphorylation alterations in PACS1$^{(+/R203W)}$, most dysregulated
380 processes converged. We observed upregulation of processes related to axonogenesis and
381 synapse maturation, suggesting accelerated development in PACS1$^{(+/R203W)}$ organoids. However,
382 although the PACS1$^{(+/R203W)}$ organoids presented with early synaptic formation signatures, the
383 regulation of multiple synapse and vesicle-related proteins are affected and many synaptic
384 maturation processes are lost, possibly disrupting proper synaptic function. This is consistent with
385 the observed phenotype in mice overexpressing PACS1 p.R203W (22); and the asynchrony and
386 an increased network burst duration reported in neurons harboring the p.R203W derived from
387 patient iPSC lines (23). Interestingly the synaptic terms obtained from protein abundance and
388 phosphorylation were also obtained from transcriptomic data, suggesting that the PACS1
389 p.R203W variant might affect multiple regulatory levels.

390 Proteomic approaches are usually bulk and lack single-cell resolution, our experimental
391 set up also lacks cells that emerge later in development (astrocytes and oligodendrocytes) or
392 arise from non-ectoderm layers (microglia). Other model systems should be explored to determine
393 how these cells contribute to PACS1 syndrome pathogenesis. Nevertheless, we identified multiple
394 proteins that displayed temporal changes in abundance and phosphorylation status in developing
395 PACS1$^{(+/R203W)}$ brain organoids with respect to controls. Interestingly, most proteins that we found
396 dysregulated in PACS1$^{(+/R203W)}$ organoids have also been linked to NDDs (63-65). Further
397 mechanistic analysis is required, however, to understand if these effects are direct or indirect.

398 Most proteins that lost their upregulation over time, and their resulting dysregulated
399 processes, could be linked to known PACS1 functions. For example, PACS1's role in protein
400 sorting explains the overrepresentation of vesicle-related processes in the up-stable cluster.

401 Moreover, many established PACS1 interactors were uncovered as dysregulated proteins were
402 not only related to known PACS1 functions but also to several known PACS1 interactors, such
403 as its close paralog, PACS2. PACS1 and PACS2 evolutionarily emerged as a duplication in higher
404 metazoans from an ancient PACS gene (66). PACS1 function primarily involves sorting from
405 endosomes to the tGN and is dependent on AP-1 and AP-3 clathrin adaptors (which also showed
406 decreased abundance over time in PACS1$^{(+/R203W)}$ organoids) (15). Meanwhile, PACS2 evolved
407 cargo-sorting functions from the Golgi to ER and vesicular coat preference for COPII. We detected
408 a gain of PACS2 regulation through increased phosphorylation at S437, which favors PACS2
409 trafficking function (47). Thus, this increased phosphorylated PACS2 could explain the
410 dysregulated vesicle trafficking and upregulation of the COPII-coated vesicle budding in the Golgi
411 transport observed in PACS1$^{(+/R203W)}$ organoids. On the other hand, it could also explain the
412 observed loss of upregulation of apoptotic proteins (Figure 2C). Interestingly, a recurrent *de novo*
413 missense mutation in the regulatory middle region of PACS2 is associated with PACS2
414 Syndrome, another NDD (67). Further research aimed to understand the interconnection of
415 PACS1 and PACS2 function, as well as their dysregulation and compensatory effects in disease,
416 will help shed light on the pathogenesis of both PACS1 and PACS2 syndromes.

417 The processes that lost downregulation over time were related to recently described
418 PACS1 functions, including proteins related to the maintenance of genome stability and DNA
419 repair via interaction with HDAC2, HDAC3, and HDAC6 (20, 22). Although we did not observe
420 protein abundance and phosphorylation status changes in HDAC2, 3, or 6, we found that HDAC5
421 gain upregulation and HDAC1 had decreased phosphorylation over maturation. This is consistent
422 with the possible pathogenic interaction between PACS1 p.R203W and HDAC6 (22). HDAC1
423 interacts with RB1 and SMARCA4 (both dysregulated at the phosphorylation level) in a repressive
424 complex in resting neurons that is abolished in a calcium-dependent manner to enable
425 transcription (68). This suggests that the PACS1 p.R203W variant could affect transcription
426 regulation by destabilizing the repressive complex formed by HDAC1, RB1, and SMARCA4.

427 Processes unrelated to known PACS1 functions also emerged, like the enrichment in
428 cluster down-stable associated to regulating protein translation. Although there is growing
429 evidence of the impact of protein translation on the pathogenesis of neurodevelopmental
430 disorders including ASD and fragile X syndrome (69), this is the first time it has been implicated
431 in PACS1 syndrome pathogenesis. Moreover, PACS1$^{(+/R203W)}$ organoids presented with changes
432 in genes reported to also be dysregulated in other neurological diseases. The presence of the
433 PACS1 p.R203W variant, at the proteomic level, seems to affect processes related to the clinical
434 features that patients manifest, including ASD, ID, and seizures (3, 56), as well as phenotypes
435 yet to be reported like neurodegeneration. Additional models are required to test mechanisms of
436 PACS1 syndrome outside the cerebral cortex, like the observed hypoplasia of the cerebellum and
437 the corpus callosum, or the dysmorphic facial features.

438 The processes that seem unrelated to PACS1 function but with observed upregulation in
439 the PACS1$^{(+/R203W)}$ organoids should be further explored. Because current evidence suggests that
440 the PACS1 p.R203W pathogenic variant could result in a gain of function (22, 23, 70), there is
441 increased interest in generating targeted therapeutic strategies aimed to suppress its toxic effects
442 (22, 26). Thus, the processes that seem unrelated to PACS1 function but with observed
443 upregulation in the PACS1$^{(+/R203W)}$ organoids should be further explored. Understanding whether
444 the proteomic dysregulation results from the toxicity associated to the variant or as a
445 compensatory mechanism to maintain cellular homeostasis would be especially relevant. Finally,
446 the neurological phenotypes associated with dysregulated protein abundance and
447 phosphorylation in PACS1 p.R203W organoids are consistent with clinical characteristics
448 observed in PACS1 syndrome patients. Further downstream analyses into understanding the
449 converging dysregulated processes could offer novel therapeutic strategies for PACS1 syndrome.
450 Our results highlight that proteomic analyses not only enhance our understanding of general NDD
451 mechanisms by complementing transcriptomic studies, but also could uncover additional targets,
452 facilitating therapy development.

***Acknowledgements***

This research was supported in part through the computational resources and staff contributions provided for the Quest high performance computing facility at Northwestern University which is jointly supported by the Office of the Provost, the Office for Research, and Northwestern University Information Technology.

***Authors' contributions***

This work was conceptualized by AGG. XGM performed proteomics analysis with help from SR, BD, JG, and MLM, and generated the figures with the help of AW. LR cultured the organoids, collected samples, and prepared them for proteomic analysis. AW, ALS, and JR performed wet lab experiments (immunohistochemistry, imaging) and data analysis. Writing was done by XGM and edited by AGG, MLM, LR, JR and ALS. All authors read and approved the final manuscript.

***Funding***

This work was funded by the PACS1 Syndrome Research Foundation (AGG) and by National Institutes of Health NINDS R01NS123163 (AGG) as well as R01MH125235 (M.L.M and B.D.), R01MH118497 (MLM). Confocal microscopy was done at the Northwestern University Center for Advanced Microscopy funded by NCI CCSG P30 CA060553.

***Competing interests***

The authors have nothing to disclose.

***Availability of data and materials***

Data is provided within the manuscript or supplementary information files and from the corresponding author on reasonable request.

481 **References**


482 1. Castellani CA, Arking DE. High-Risk, High-Reward Genetics in ASD. Neuron.
483 2020;105(3):407-10.
484 2. Geschwind DH, Flint J. Genetics and genomics of psychiatric disease. Science.
485 2015;349(6255):1489-94.
486 3. Schuurs-Hoeijmakers JH, Landsverk ML, Foulds N, Kukolich MK, Gavrilova RH,
487 Greville-Heygate S, et al. Clinical delineation of the PACS1-related syndrome--Report on 19
488 patients. Am J Med Genet A. 2016;170(3):670-5.
489 4. Schuurs-Hoeijmakers JH, Oh EC, Vissers LE, Swinkels ME, Gilissen C, Willemsen MA,
490 et al. Recurrent de novo mutations in PACS1 cause defective cranial-neural-crest migration and
491 define a recognizable intellectual-disability syndrome. Am J Hum Genet. 2012;91(6):1122-7.
492 5. Seto MT, Bertoli-Avella AM, Cheung KW, Chan KY, Yeung KS, Fung JL, et al. Prenatal
493 and postnatal diagnosis of Schuurs-Hoeijmakers syndrome: Case series and review of the
494 literature. Am J Med Genet A. 2021;185(2):384-9.
495 6. Thomas G, Aslan JE, Thomas L, Shinde P, Shinde U, Simmen T. Caught in the act -
496 protein adaptation and the expanding roles of the PACS proteins in tissue homeostasis and
497 disease. J Cell Sci. 2017;130(11):1865-76.
498 7. Scott GK, Gu F, Crump CM, Thomas L, Wan L, Xiang Y, et al. The phosphorylation state
499 of an autoregulatory domain controls PACS-1-directed protein traffic. EMBO J.
500 2003;22(23):6234-44.
501 8. Wan L, Molloy SS, Thomas L, Liu G, Xiang Y, Rybak SL, et al. PACS-1 defines a novel
502 gene family of cytosolic sorting proteins required for trans-Golgi network localization. Cell.
503 1998;94(2):205-16.
504 9. Crump CM, Xiang Y, Thomas L, Gu F, Austin C, Tooze SA, et al. PACS-1 binding to
505 adaptors is required for acidic cluster motif-mediated protein traffic. EMBO J. 2001;20(9):2191-
506 201.
507 10. Hinners I, Wendler F, Fei H, Thomas L, Thomas G, Tooze SA. AP-1 recruitment to
508 VAMP4 is modulated by phosphorylation-dependent binding of PACS-1. EMBO Rep.
509 2003;4(12):1182-9.
510 11. Gu F, Crump CM, Thomas G. Trans-Golgi network sorting. Cell Mol Life Sci.
511 2001;58(8):1067-84.
512 12. Molloy SS, Thomas L, Kamibayashi C, Mumby MC, Thomas G. Regulation of endosome
513 sorting by a specific PP2A isoform. J Cell Biol. 1998;142(6):1399-411.
514 13. Schermer B, Hopker K, Omran H, Ghenoiu C, Fliegauf M, Fekete A, et al.
515 Phosphorylation by casein kinase 2 induces PACS-1 binding of nephrocystin and targeting to
516 cilia. EMBO J. 2005;24(24):4415-24.
517 14. Jenkins PM, Zhang L, Thomas G, Martens JR. PACS-1 mediates phosphorylation-
518 dependent ciliary trafficking of the cyclic-nucleotide-gated channel in olfactory sensory neurons.
519 J Neurosci. 2009;29(34):10541-51.
520 15. Kottgen M, Benzing T, Simmen T, Tauber R, Buchholz B, Feliciangeli S, et al. Trafficking
521 of TRPP2 by PACS proteins represents a novel mechanism of ion channel regulation. EMBO J.
522 2005;24(4):705-16.
523 16. Gorini G, Ponomareva O, Shores KS, Person MD, Harris RA, Mayfield RD. Dynamin-1
524 co-associates with native mouse brain BKCa channels: proteomics analysis of synaptic protein
525 complexes. FEBS Lett. 2010;584(5):845-51.
526 17. Taya S, Shinoda T, Tsuboi D, Asaki J, Nagai K, Hikita T, et al. DISC1 regulates the
527 transport of the NUDEL/LIS1/14-3-3epsilon complex through kinesin-1. J Neurosci.
528 2007;27(1):15-26.
529 18. Liu H, Hu PW, Budhiraja S, Misra A, Couturier J, Lloyd RE, et al. PACS1 is an HIV-1
530 cofactor that functions in Rev-mediated nuclear export of viral RNA. Virology. 2020;540:88-96.

19. Atkins KM, Thomas LL, Barroso-Gonzalez J, Thomas L, Auclair S, Yin J, et al. The multifunctional sorting protein PACS-2 regulates SIRT1-mediated deacetylation of p53 to modulate p21-dependent cell-cycle arrest. Cell Rep. 2014;8(5):1545-57.
20. Mani C, Tripathi K, Luan S, Clark DW, Andrews JF, Vindigni A, et al. The multifunctional protein PACS-1 is required for HDAC2- and HDAC3-dependent chromatin maturation and genomic stability. Oncogene. 2020;39(12):2583-96.
21. Veena MS, Raychaudhuri S, Basak SK, Venkatesan N, Kumar P, Biswas R, et al. Dysregulation of hsa-miR-34a and hsa-miR-449a leads to overexpression of PACS-1 and loss of DNA damage response (DDR) in cervical cancer. J Biol Chem. 2020;295(50):17169-86.
22. Villar-Pazos S, Thomas L, Yang Y, Chen K, Lyles JB, Deitch BJ, et al. Neural deficits in a mouse model of PACS1 syndrome are corrected with PACS1- or HDAC6-targeting therapy. Nat Commun. 2023;14(1):6547.
23. Rylaarsdam L, Rakotomamonjy J, Pope E, Guemez-Gamboa A. iPSC-derived models of PACS1 syndrome reveal transcriptional and functional deficits in neuron activity. Nat Commun. 2024;15(1):827.
24. Byrd DT, Han ZC, Piggott CA, Jin Y. PACS-1 variant protein is aberrantly localized in Caenorhabditis elegans model of PACS1/PACS2 syndromes. Genetics. 2024;228(2).
25. Van Nuland A, Reddy T, Quassem F, Vassalli JD, Berg AT. PACS1-Neurodevelopmental disorder: clinical features and trial readiness. Orphanet J Rare Dis. 2021;16(1):386.
26. Rylaarsdam L, Reddy T, Guemez-Gamboa A. In search of a cure: PACS1 Research Foundation as a model of rare disease therapy development. Trends Genet. 2022;38(2):109-12.
27. Melliou S, Sangster KT, Djuric U, Diamandis P. The promise of organoids for unraveling the proteomic landscape of the developing human brain. Mol Psychiatry. 2022;27(1):73-80.
28. Li C, Fleck JS, Martins-Costa C, Burkard TR, Themann J, Stuempflen M, et al. Single-cell brain organoid screening identifies developmental defects in autism. Nature. 2023;621(7978):373-80.
29. Paulsen B, Velasco S, Kedaigle AJ, Pigoni M, Quadrato G, Deo AJ, et al. Autism genes converge on asynchronous development of shared neuron classes. Nature. 2022;602(7896):268-73.
30. Buccitelli C, Selbach M. mRNAs, proteins and the emerging principles of gene expression control. Nat Rev Genet. 2020;21(10):630-44.
31. Sloan SA, Andersen J, Pasca AM, Birey F, Pasca SP. Generation and assembly of human brain region-specific three-dimensional cultures. Nat Protoc. 2018;13(9):2062-85.
32. Dumrongprechachan V, Salisbury RB, Butler L, MacDonald ML, Kozorovitskiy Y. Dynamic proteomic and phosphoproteomic atlas of corticostriatal axons in neurodevelopment. Elife. 2022;11.
33. Plubell DL, Wilmarth PA, Zhao Y, Fenton AM, Minnier J, Reddy AP, et al. Extended Multiplexing of Tandem Mass Tags (TMT) Labeling Reveals Age and High Fat Diet Specific Proteome Changes in Mouse Epididymal Adipose Tissue. Mol Cell Proteomics. 2017;16(5):873-90.
34. Ritchie ME, Phipson B, Wu D, Hu Y, Law CW, Shi W, et al. limma powers differential expression analyses for RNA-sequencing and microarray studies. Nucleic Acids Res. 2015;43(7):e47.
35. Ernst J, Bar-Joseph Z. STEM: a tool for the analysis of short time series gene expression data. BMC Bioinformatics. 2006;7:191.
36. Djuric U, Lam KHB, Kao J, Batruch I, Jevtic S, Papaioannou MD, et al. Defining Protein Pattern Differences Among Molecular Subtypes of Diffuse Gliomas Using Mass Spectrometry. Mol Cell Proteomics. 2019;18(10):2029-43.
37. Shen L, Sinai M. GeneOverlap: Test and visualize gene overlaps. R package version. 2013;1(0):444.

582 38. Gehlenborg N. UpSetR: a more scalable alternative to Venn and Euler diagrams for
583 visualizing intersecting sets. R package version. 2019;1(0).
584 39. Zhou Y, Zhou B, Pache L, Chang M, Khodabakhshi AH, Tanaseichuk O, et al.
585 Metascape provides a biologist-oriented resource for the analysis of systems-level datasets. Nat
586 Commun. 2019;10(1):1523.
587 40. Sayols S. rrvgo: a Bioconductor package for interpreting lists of Gene Ontology terms.
588 MicroPubl Biol. 2023;2023.
589 41. Ashburner M, Ball CA, Blake JA, Botstein D, Butler H, Cherry JM, et al. Gene ontology:
590 tool for the unification of biology. The Gene Ontology Consortium. Nat Genet. 2000;25(1):25-9.
591 42. Gene Ontology C, Aleksander SA, Balhoff J, Carbon S, Cherry JM, Drabkin HJ, et al.
592 The Gene Ontology knowledgebase in 2023. Genetics. 2023;224(1).
593 43. Pinero J, Ramirez-Anguita JM, Sauch-Pitarch J, Ronzano F, Centeno E, Sanz F, et al.
594 The DisGeNET knowledge platform for disease genomics: 2019 update. Nucleic Acids Res.
595 2020;48(D1):D845-D55.
596 44. Moon K, Martino T. R Package 'webr': Data and Functions for Web-Based Analysis. R
597 package version 01. 2020;5.
598 45. Wickham H. ggplot2: Elegant Graphics for Data Analysis. Springer-Verlag New York;
599 2106.
600 46. Shannon P, Markiel A, Ozier O, Baliga NS, Wang JT, Ramage D, et al. Cytoscape: a
601 software environment for integrated models of biomolecular interaction networks. Genome Res.
602 2003;13(11):2498-504.
603 47. Banerjee-Basu S, Packer A. SFARI Gene: an evolving database for the autism research
604 community. Dis Model Mech. 2010;3(3-4):133-5.
605 48. Anastasaki C, Wegscheid ML, Hartigan K, Papke JB, Kopp ND, Chen J, et al. Human
606 iPSC-Derived Neurons and Cerebral Organoids Establish Differential Effects of Germline NF1
607 Gene Mutations. Stem Cell Reports. 2020;14(4):541-50.
608 49. Hruska M, Dalva MB. Ephrin regulation of synapse formation, function and plasticity. Mol
609 Cell Neurosci. 2012;50(1):35-44.
610 50. Cho Y, Cavalli V. HDAC5 is a novel injury-regulated tubulin deacetylase controlling axon
611 regeneration. EMBO J. 2012;31(14):3063-78.
612 51. Foley K, McKee C, Nairn AC, Xia H. Regulation of Synaptic Transmission and Plasticity
613 by Protein Phosphatase 1. J Neurosci. 2021;41(14):3040-50.
614 52. Scott GK, Fei H, Thomas L, Medigeshi GR, Thomas G. A PACS-1, GGA3 and CK2
615 complex regulates CI-MPR trafficking. EMBO J. 2006;25(19):4423-35.
616 53. Deng L, Ding L, Duan X, Peng Y. Shared molecular signatures between coronavirus
617 infection and neurodegenerative diseases provide targets for broad-spectrum drug
618 development. Sci Rep. 2023;13(1):5457.
619 54. Ciani L, Boyle KA, Dickins E, Sahores M, Anane D, Lopes DM, et al. Wnt7a signaling
620 promotes dendritic spine growth and synaptic strength through Ca(2)(+)/Calmodulin-dependent
621 protein kinase II. Proc Natl Acad Sci U S A. 2011;108(26):10732-7.
622 55. Aber R, Chan W, Mugisha S, Jerome-Majewska LA. Transmembrane emp24 domain
623 proteins in development and disease. Genet Res (Camb). 2019;101:e14.
624 56. Aslan JE, You H, Williamson DM, Endig J, Youker RT, Thomas L, et al. Akt and 14-3-3
625 control a PACS-2 homeostatic switch that integrates membrane traffic with TRAIL-induced
626 apoptosis. Mol Cell. 2009;34(4):497-509.
627 57. Pflum MK, Tong JK, Lane WS, Schreiber SL. Histone deacetylase 1 phosphorylation
628 promotes enzymatic activity and complex formation. J Biol Chem. 2001;276(50):47733-41.
629 58. Tsukada M, Prokscha A, Ungewickell E, Eichele G. Doublecortin association with actin
630 filaments is regulated by neurabin II. J Biol Chem. 2005;280(12):11361-8.
631 59. Cesca F, Baldelli P, Valtorta F, Benfenati F. The synapsins: key actors of synapse
632 function and plasticity. Prog Neurobiol. 2010;91(4):313-48.

633 60. Nakatsu F, Ohno H. Adaptor protein complexes as the key regulators of protein sorting
634 in the post-Golgi network. Cell Struct Funct. 2003;28(5):419-29.
635 61. Srinivasan S, Burckhardt CJ, Bhave M, Chen Z, Chen PH, Wang X, et al. A
636 noncanonical role for dynamin-1 in regulating early stages of clathrin-mediated endocytosis in
637 non-neuronal cells. PLoS Biol. 2018;16(4):e2005377.
638 62. Gu Y, Hamajima N, Ihara Y. Neurofibrillary tangle-associated collapsin response
639 mediator protein-2 (CRMP-2) is highly phosphorylated on Thr-509, Ser-518, and Ser-522.
640 Biochemistry. 2000;39(15):4267-75.
641 63. Andreu-Cervera A, Catala M, Schneider-Maunoury S. Cilia, ciliopathies and hedgehog-
642 related forebrain developmental disorders. Neurobiol Dis. 2021;150:105236.
643 64. Cho J, Chang H, Kwon SC, Kim B, Kim Y, Choe J, et al. LIN28A is a suppressor of ER-
644 associated translation in embryonic stem cells. Cell. 2012;151(4):765-77.
645 65. Tenorio-Castano J, Morte B, Nevado J, Martinez-Glez V, Santos-Simarro F, Garcia-
646 Minaur S, et al. Schuurs-Hoeijmakers Syndrome (PACS1 Neurodevelopmental Disorder):
647 Seven Novel Patients and a Review. Genes (Basel). 2021;12(5).
648 66. Parikshak NN, Luo R, Zhang A, Won H, Lowe JK, Chandran V, et al. Integrative
649 functional genomic analyses implicate specific molecular pathways and circuits in autism. Cell.
650 2013;155(5):1008-21.
651 67. Sanders SJ, Murtha MT, Gupta AR, Murdoch JD, Raubeson MJ, Willsey AJ, et al. De
652 novo mutations revealed by whole-exome sequencing are strongly associated with autism.
653 Nature. 2012;485(7397):237-41.
654 68. Jourdon A, Scuderi S, Capauto D, Abyzov A, Vaccarino FM. PsychENCODE and
655 beyond: transcriptomics and epigenomics of brain development and organoids.
656 Neuropsychopharmacology. 2021;46(1):70-85.
657 69. Zhao X, Bhattacharyya A. Human Models Are Needed for Studying Human
658 Neurodevelopmental Disorders. Am J Hum Genet. 2018;103(6):829-57.
659 70. Nascimento JM, Saia-Cereda VM, Sartore RC, da Costa RM, Schitine CS, Freitas HR,
660 et al. Human Cerebral Organoids and Fetal Brain Tissue Share Proteomic Similarities. Front
661 Cell Dev Biol. 2019;7:303.
662 71. Nascimento JM, Saia-Cereda VM, Zuccoli GS, Reis-de-Oliveira G, Carregari VC, Smith
663 BJ, et al. Proteomic signatures of schizophrenia-sourced iPSC-derived neural cells and brain
664 organoids are similar to patients' postmortem brains. Cell Biosci. 2022;12(1):189.
665 72. Banerjee S, Zhao Q, Wang B, Qin J, Yuan X, Lou Z, et al. A novel in-frame deletion in
666 KIF5C gene causes infantile onset epilepsy and psychomotor retardation. MedComm (2020).
667 2024;5(4):e469.
668 73. Granata A, Watson R, Collinson LM, Schiavo G, Warner TT. The dystonia-associated
669 protein torsinA modulates synaptic vesicle recycling. J Biol Chem. 2008;283(12):7568-79.
670 74. Halperin D, Kadir R, Perez Y, Drabkin M, Yogev Y, Wormser O, et al. SEC31A mutation
671 affects ER homeostasis, causing a neurological syndrome. J Med Genet. 2019;56(3):139-48.
672 75. Youker RT, Shinde U, Day R, Thomas G. At the crossroads of homoeostasis and
673 disease: roles of the PACS proteins in membrane traffic and apoptosis. Biochem J.
674 2009;421(1):1-15.
675 76. Olson HE, Jean-Marcais N, Yang E, Heron D, Tatton-Brown K, van der Zwaag PA, et al.
676 A Recurrent De Novo PACS2 Heterozygous Missense Variant Causes Neonatal-Onset
677 Developmental Epileptic Encephalopathy, Facial Dysmorphism, and Cerebellar Dysgenesis. Am
678 J Hum Genet. 2018;103(4):631.
679 77. Qiu Z, Ghosh A. A calcium-dependent switch in a CREST-BRG1 complex regulates
680 activity-dependent gene expression. Neuron. 2008;60(5):775-87.
681 78. Jishi A, Qi X, Miranda HC. Implications of mRNA translation dysregulation for
682 neurological disorders. Semin Cell Dev Biol. 2021;114:11-9.

683 79. Liu Y, Ding H, Yan T, Liu L, Yu L, Huang Y, et al. A Novel Multi-Exon Deletion of PACS1
684 in a Three-Generation Pedigree: Supplements to PACS1 Neurodevelopmental Disorder
685 Spectrum. Front Genet. 2021;12:690216.

686

687

688 **Figures**

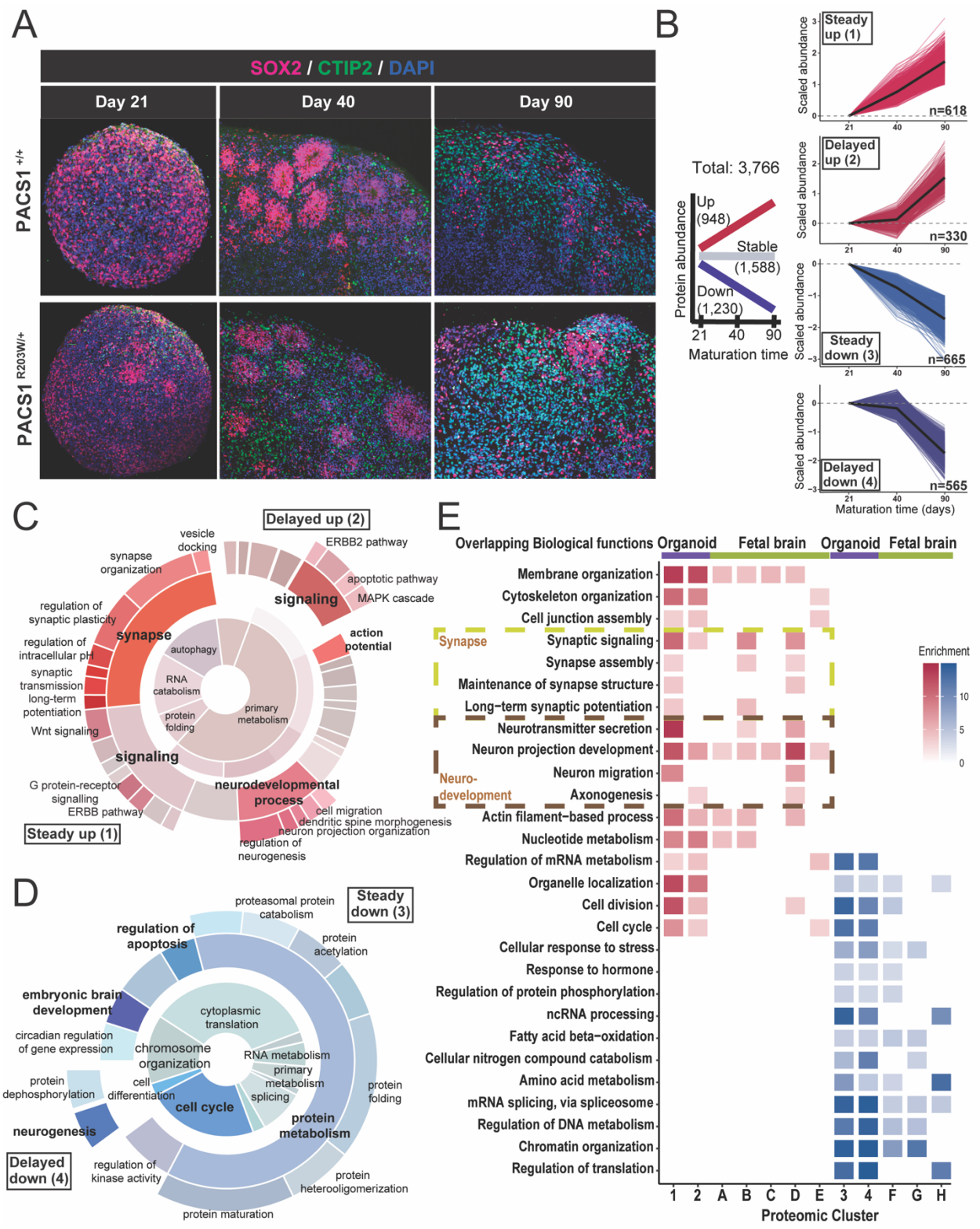


689

690 **Figure 1. Cortical organoids recapitulate proteome dynamics during brain development.**
691 A) Expression of neural precursor protein SOX2 (red) and projection neuron marker CTIP2
692 (magenta) in day 21, 40, and 80 organoids derived from control (up) and PACS1 p.R203W
693 organoids (bottom). Scale bar = 100 µm. DAPI (blue) B) Total proteins detected in organoids were
694 clustered by abundance changes over maturation time into three major trends: upregulated (red),
695 downregulated (blue) or stable (gray) (graph on the left). Further classification detected four main
696 abundance trends, based on the timing of change: steady over time (clusters steady -up and -
697 down), or delayed to day 40 (clusters delayed -up and -down) (Right). Total number of proteins
698 assigned to a cluster are indicated in each graph. C, D) Top GO terms upregulated (red) and
699 downregulated (blue) by cluster over maturation time. The inner pie plots represent processes
700 common to the clusters in each panel. The nested pie charts show root and branch significant
701 GO enrichments with the width of the pie correlating to -log(p) of the GO term. Neurodevelopment-
702 related processes (bold). E) Top GO terms upregulated (red) and downregulated (blue) shared
703 between organoids (purple) and fetal brain (green) over time. Synapse and neurodevelopment-
704 related processes (box). Organoid profiles correspond to clusters 1 to 4, while the fetal brain
705 profiles correspond to clusters A to H. A full description of all enriched processes is included in
706 Supplementary Table 9.
707

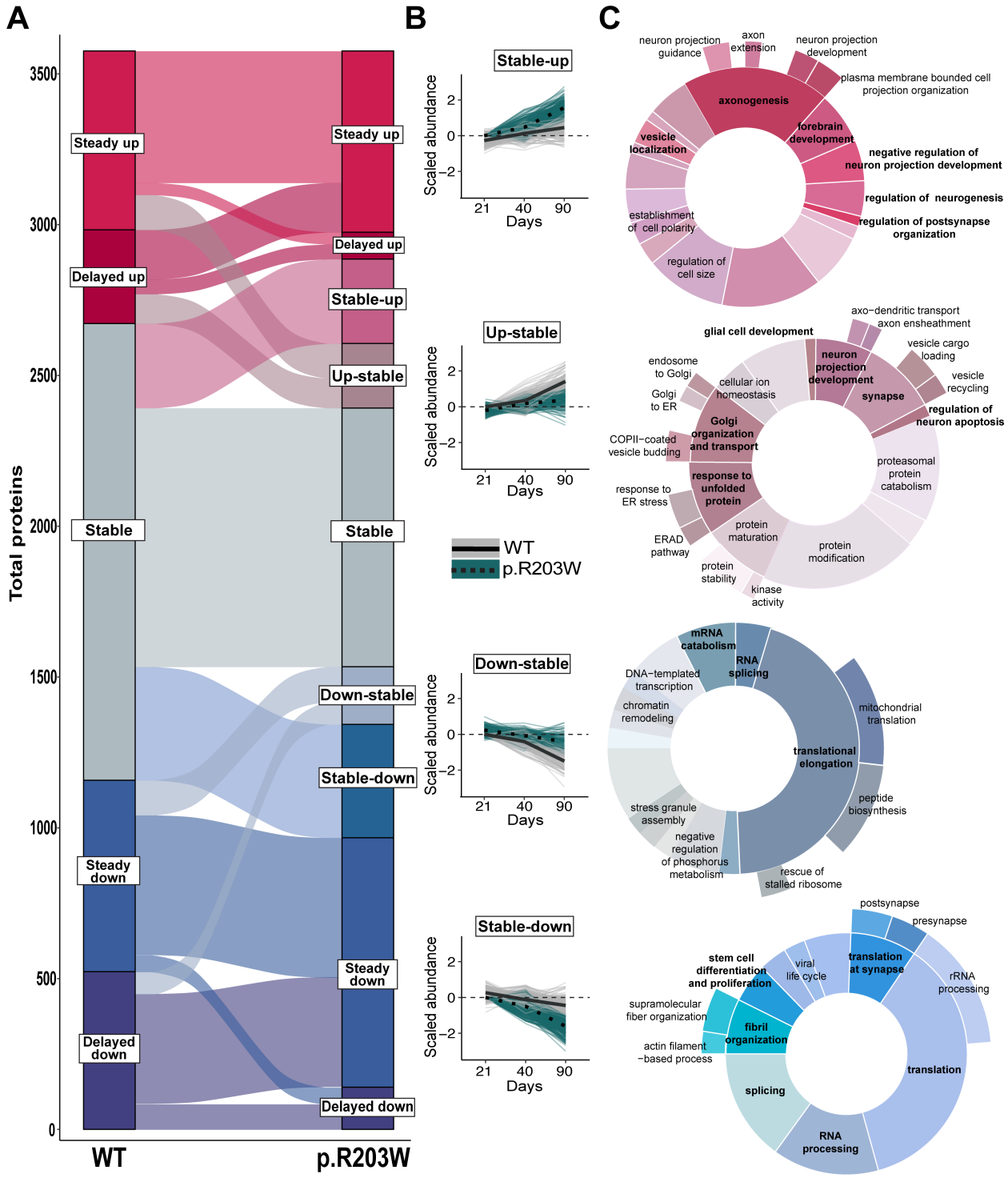


**Figure 2. Organoids carrying the PACS1 p.R203W pathogenic variant present with altered protein dynamics during maturation.** A) Alluvial plot indicating the change of profile clustering in the PACS1 p.R203W organoids (right) in contrast to the clustering in controls (left). B) Four

712 clusters of dysregulated proteins were identified in PACS1 p.R203W organoids. The plots are
713 organized into a gain or loss of regulation categories: cluster stable-up (top, red), and stable-down
714 (bottom, blue) gained regulation while clusters up- and down-stable lost regulation (middle, grey
715 tones), C) Enriched biological functions per dysregulated cluster. The nested pie charts show root
716 and branch significant GO enrichments and the width of the pie correlating to -log(p) of the GO
717 term. Neurodevelopment-related processes (bold).

718

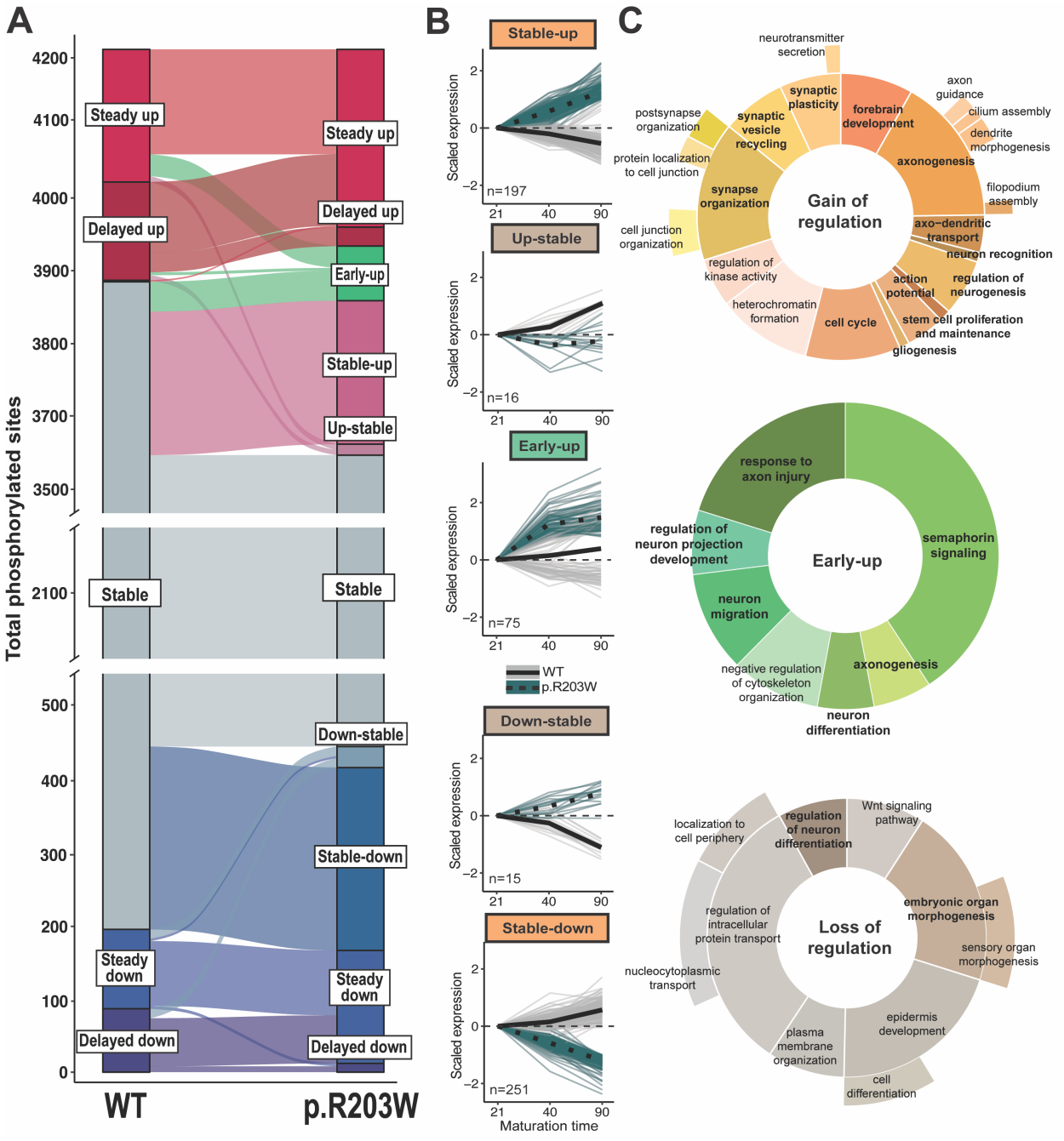


**Figure 3. Dysregulation of temporal phosphorylation dynamics in PACS1 p.R203W organoids.** A) Alluvial plot indicating the change of profile clustering in the PACS1 p.R203W organoids in contrast to controls. Breaks in the y axis were introduced to improve visualization of the dysregulated clusters by removing 3,000 modifications that remained stable over time. B) Five clusters of dysregulated phosphorylation trends were observed in PACS1 p.R203W organoids

725 that either gained a temporal regulation or lost the original pattern observed in the controls. The
726 plots are organized into a gain or loss of regulation categories: clusters stable- up and -down
727 gained temporal regulation in contrast to the controls (orange), while clusters up- and down-
728 stable lost temporal regulation (gray). Early-up is a new cluster exclusive to the phosphorylation
729 dataset that also gained temporal regulation (green). C) Enriched biological functions per
730 dysregulated cluster. The nested pie charts show root and branch significant GO enrichments
731 and the width of the pie correlating to -log(p) of the GO term. Neurodevelopment-related
732 processes (bold).

733

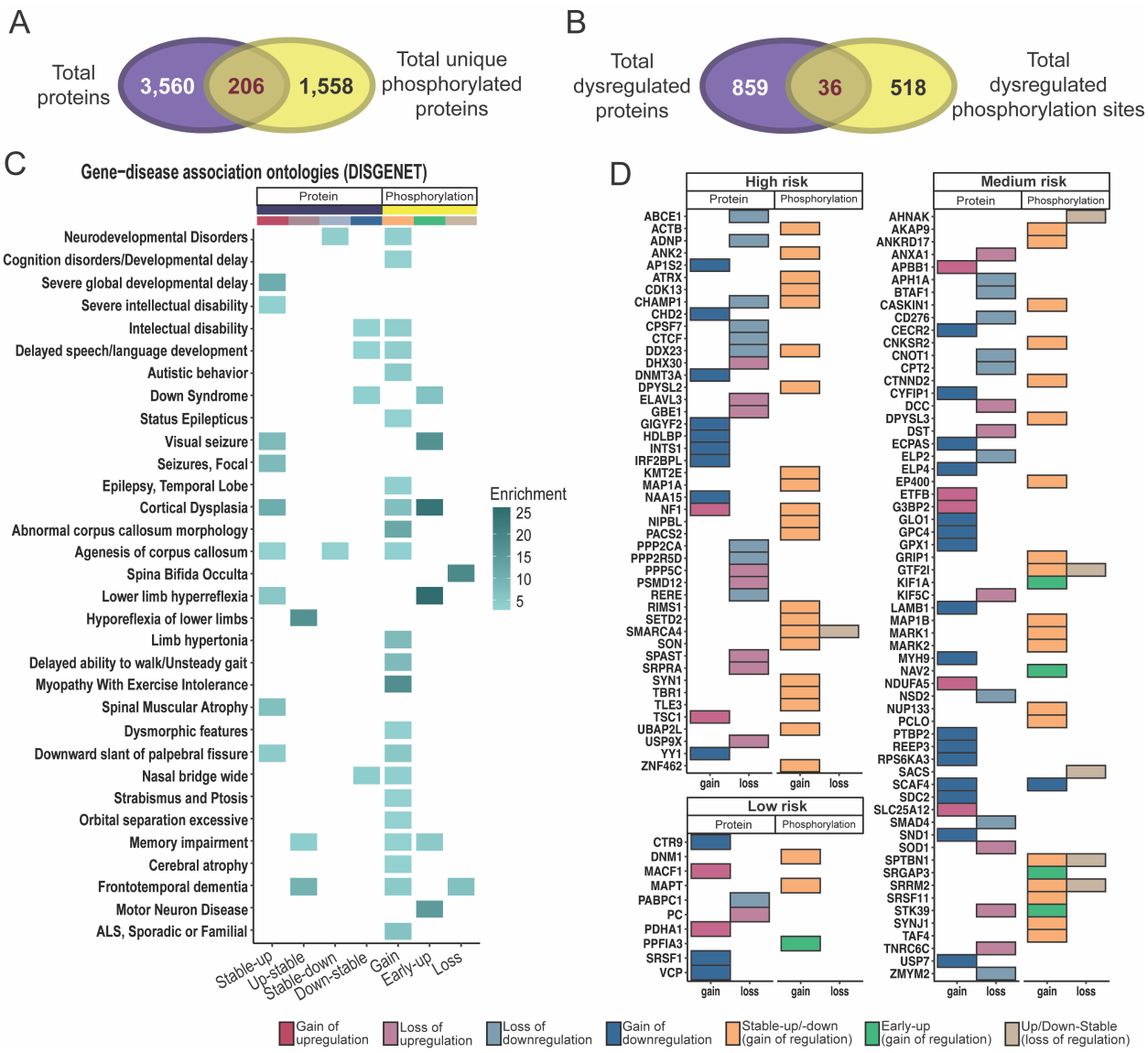


**Figure 4. Protein abundance and phosphorylation sites dysregulated by PACS1 p.R203W are enriched in neurological disease-related genes.** A) Overlapping identities between all detected proteins and proteins with identified phosphorylation sites. B) Overlapping identities between dysregulated proteins and phosphorylation sites observed in the PACS1 p.R203W organoids when compared to controls. C) Gene-disease association type ontologies enriched in the PACS1 p.R203W dysregulated proteome (yellow) and phosphorylation sites (purple). Selected top neuro-related categories at a corrected p-value of 0.01. D) ASD risk genes dysregulated in organoids carrying the p.R203W pathogenic variant. Genes are grouped into the

743 three risk level categories determined by the SFARI database (2024 Q3 release). For both panels,
744 the protein abundance and phosphorylation clusters are organized by major dysregulation trend
745 (gain or loss) with red representing upregulation and blue representing downregulation for the
746 protein abundance clusters. The phosphorylation clusters are grouped by major trend of
747 dysregulation presented in figure 3: gain of regulation (clusters stable- up and -down) or loss of
748 regulation (clusters up- and down- stable), as well as cluster early-up, exclusive of the
749 dysregulated phosphorylation sites.
750

751 **Supplemental Material**

752 **Supplementary information.** Supplementary Methods and supplementary figures 1-4 containing
753 additional data.

754 **Supplementary tables.** Supplementary Tables 1-20 containing the list of proteins and
755 phosphorylation sites, as well as accompanying statistical analysis performed on the data.